JUSTC

Article

http://justc.ustc.edu.cn

Received: May 10, 2024; Accepted: June 18, 2024

Effects of the oxygen transport properties of electrolytes on the reaction mechanisms in lithium–oxygen batteries

Aijing Yan, Zhuojun Zhang, Xu Xiao ✉, and Peng Tan ✉

Department of Thermal Science and Energy Engineering, University of Science and Technology of China, Hefei 230026, China

✉Correspondence: Xu Xiao, E-mail: xiaoxu@ustc.edu.cn; Peng Tan, E-mail: pengtan@ustc.edu.cn

© 2025 The Author(s). This is an open access article under the CC BY-NC-ND 4.0 license (http://creativecommons.org/licenses/by-nc-nd/4.0/).

Graphical abstract

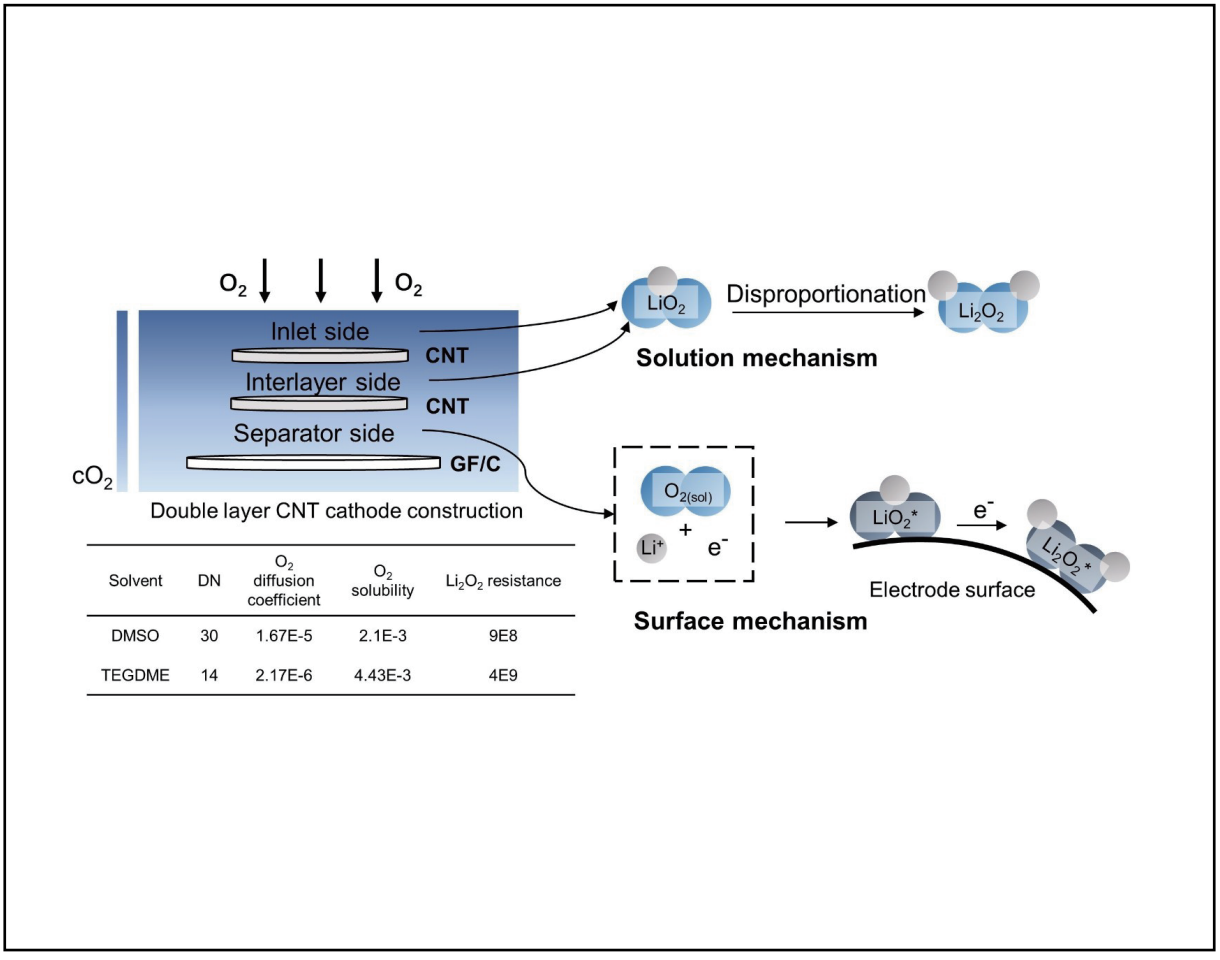

Solvent	DN	O_2 diffusion coefficient	O_2 solubility	Li_2O_2 resistance
DMSO	30	1.67E-5	2.1E-3	9E8
TEGDME	14	2.17E-6	4.43E-3	4E9

The reaciton mechanism varying with the oxygen concentration.

Public summary

■ The importance of mass transport is emphasized by the use of a two-layer electrode.

■ The effects of the oxygen transport properties of electrolytes on battery performance are revealed.

■ A novel reaction mechanism that varies with the spatial position of the electrode is proposed.

Citation: Yan A J, Zhang Z J, Xiao X, et al. Effects of the oxygen transport properties of electrolytes on the reaction mechanisms in lithium–oxygen batteries. *JUSTC*, **2025**, 55(2): 0204. CSTR: 32290.14.JUSTC-2024-0035. DOI: 10.52396/JUSTC-2024-0035

JUSTC

Article

http://justc.ustc.edu.cn

Received: May 10, 2024; Accepted: June 18, 2024

Effects of the oxygen transport properties of electrolytes on the reaction mechanisms in lithium–oxygen batteries

Aijing Yan, Zhuojun Zhang, Xu Xiao ✉, and Peng Tan ✉

Department of Thermal Science and Energy Engineering, University of Science and Technology of China, Hefei 230026, China

✉Correspondence: Xu Xiao, E-mail: xiaoxu@ustc.edu.cn; Peng Tan, E-mail: pengtan@ustc.edu.cn
© 2025 The Author(s). This is an open access article under the CC BY-NC-ND 4.0 license (http://creativecommons.org/licenses/by-nc-nd/4.0/).

Cite This: *JUSTC*, **2025**, 55(2): 0204 (8pp)

Read Online

Abstract: Lithium–oxygen batteries attract considerable attention due to exceptionally high theoretical energy density, while the development remains in its early stage. As is widely suggested, the solution mechanism induces greater discharge capacity, while the surface mechanism induces greater cycle stability. Therefore, battery performance can be improved by adjusting the reaction mechanism. Previous studies predominantly focus on extremely thin or flat electrodes. In contrast, this work utilizes thick electrodes, emphasizing the importance of mass transport. Given that the electrolyte solvent is the main site of mass transport, the effects of two typical solvents on mass transport and battery performance are investigated: dimethyl sulfoxide with low viscosity and a high O_2 diffusion rate and tetraethylene glycol dimethyl ether with high O_2 solubility and high Li^+ transport capability. The results reveal a novel pathway for reaction mechanism induction where the mechanism varies with the spatial position of the electrode. As the spatial distribution of the electrode progresses, a layered appearance of solution mechanism products, transition state products, and surface mechanism products emerges, which is attributed to the increase in the mass transfer resistance. This work presents a distinct perspective on the way solvents influence reaction pathways and offers a new approach to regulating reaction pathways.

Keywords: Li–O_2 battery; nonaqueous electrolyte; oxygen transport property; solution mechanism; surface mechanism

CLC number: TM912 **Document code:** A

1 Introduction

As society and the economy progress, the imperative to address the environmental pollution caused by fossil fuels accentuates the urgency of developing renewable and clean energy sources. It is difficult for Li-ion batteries, which are limited by their energy density (350 Wh/kg), to meet the high energy-demanding requirements[1–4]. Owing to their high theoretical energy densities, Li–O_2 batteries (LOBs) are regarded as promising electrochemical energy storage technologies, especially for long-distance electric vehicles. Li–O_2 batteries, which are assisted by redox chemistry between Li and O_2, harvest ten times more energy density (~3600 Wh/kg) than Li-ion batteries do[5–7]. Despite being positioned as an alternative to lithium-ion batteries, the development of LOBs remains in its early stages[8–10]. Issues such as poor oxygen redox kinetics at the positive electrode[11–13], severe polarization[14,15], poor reversibility of products[16–18], and high decomposition voltage[19,20] are impeding the widespread application of LOBs. Presently, a variety of modification strategies, including the use of positive electrode catalysts[21–23], the incorporation of redox mediators (RMs)[24,25], and the application of protective layers on the anode[26,27], are widely employed to increase the battery performance of LOBs.

During the initial exploration of LOBs, successful operation of LOBs was achieved through the utilization of carbonate electrolytes[28,29]. However, the superoxide radicals generated during redox reactions in LOBs can lead to the decomposition of carbonate electrolytes, resulting in battery failure during cycling[30]. Considering the widespread application of dimethyl sulfoxide (DMSO) as a solvent, it was introduced into LOBs[1]. In addition to DMSO, ether-based solvents, such as tetraethylene glycol dimethyl ether (TEGDME), have also been extensively proven viable in LOBs[31]. In high-donor-number (DN) electrolyte solvents (such as DMSO), LiO_2 tends to dissolve in the solvent, leading to a disproportionation reaction and the formation of Li_2O_2 via the solution pathway. In low-DN solvents (such as TEGDME), voltage decay occurs rapidly, resulting in cell death attributed to the growth of Li_2O_2 films on the electrode[32,33].

In LOBs, the electrolyte solvent not only shapes the reaction pathway but also significantly influences battery performance. Johnson et al.[32] revealed the O_2 reduction mechanism of four kinds of solvents with varying DNs and reported that the solvent affects O_2 reduction by modulating the solubility of LiO_2. Christy et al.[34] explored the influence of different electrolyte solvents on the electrochemical performance. Rauter et al.[35] presented a mathematical model characterizing the impact of solvents on the reaction pathway with distinct solvents. As summarized in the work mentioned above, the solvent influences the reaction pathway through its DN value, whereas in their work, the impact of the mass transport properties of solvents is overlooked, which is attributed to their use of extremely thin or flat electrodes. Dutta et al.[36]

CSTR: 32290.14.JUSTC-2024-0035
DOI: 10.52396/JUSTC-2024-0035
JUSTC, **2025**, 55(2): 0204

investigated the rate performance and primary limiting factors of LOB through a dual-layer electrode structure. The dual-layer electrode structure extends the transport distance and facilitates the observation of internal transport phenomena within the electrodes. This work argues that the impact of solvents on the electrochemical reaction kinetics in LOB is not confined to differences in DN values alone; instead, it is also manifested in the physical properties of the solvent, including viscosity, ion conductivity, and the oxygen diffusion rate. To more significantly underscore the influence of electrolyte mass transfer coefficients on battery performance during discharge, we implemented a dual-electrode structure intended to extend transport channels and intensify mass transfer resistance, ensuring that mass transfer effects are distinctly evident on each electrode layer. Dual-layer carbon nanotubes (CNTs) were used as air electrodes. Two typical solvents, DMSO, which has a high DN, low viscosity, and high O_2 diffusion rate, and TEGDME, which has high O_2 solubility and high Li^+ transport capability, were selected for this study. This work evaluated the impact of different solvents on the morphology and distribution of discharge products on CNT electrodes and the discharge capacity, providing diverse perspectives on how solvents influence the discharge process and reaction pathways.

2 Experimental

2.1 Material preparation and battery assembly

Lithium foil (0.3 mm thick), CNT electrodes (0.06 mm thick), and glass fiber filters (GF/C, 0.26 mm thick) were purchased from China Energy Lithium Co., Ltd., Nanjing XFNANO Materials Tech Co., Ltd., and Whatman, respectively. 1 mol/L lithium bis(trifluoromethanesulfonyl)imide (LiTFSI) dissolved in TEGDME and 1 mol/L lithium perchlorate ($LiClO_4$) dissolved in DMSO were purchased from DoDoChem. All chemical reagents were used as purchased commercially without any further treatment. To measure the electrochemical performance of the Li–O_2 batteries, a Swagelok-type battery was composed of Li foil, a glass-fiber separator, and a double-layer CNT electrode with 1 mol/L LiTFSI/TEGDME (H_2O < 2E–5 by Karl Fischer titration) and 1 mol/L $LiClO_4$/DMSO (H_2O < 2E–5 by Karl Fischer titration); these materials were assembled and disassembled in an argon-atmosphere glove box (Etelux, Lab 2000, H_2O and O_2< 1E–7). The discharged batteries were disassembled in an argon-filled glove box, and the oxygen electrode was then removed, washed with dimethoxyethane (DME), and dried to remove the residual solvent. After that, the oxygen electrodes were enclosed with a thin transparent polymer film to reduce their exposure to air.

2.2 Battery tests and material characterization

After the battery assembly, O_2 (purity > 99.999%) was introduced into the battery system for 30 min to clean the argon gas. Then, the air outlet was closed, and O_2 was constantly introduced for 30 min to increase the O_2 concentration in the battery system. After that, the air inlet was closed and allowed to stand for 3 h, ensuring that O_2 dissolved into the electrolyte. The galvanostatic discharge measurements were performed on a battery cycler system (LAND BT 2000). The Li−O_2 battery was first discharged to 2.0 V at a current of 0.025 mA under pure O_2. Linear sweep voltammetry (LSV) was performed on a Solartron analyzer at a sweep rate of 0.5 mV/s at 2.0 V to 3.2 V for the LOB. The testing environment of the Swagelok-type battery was at room temperature. The crystal structure was determined via powder X-ray diffraction (XRD, Smartlab) with a Cu-Kα radiation source of 45 keV. The morphology was observed via a scanning electron microscope (SEM, XL-30 ESEM) under an accelerating voltage of 3.0 kV.

3 Results and discussion

As shown in Fig. 1a, the employed experimental setup utilizes a Swagelok battery fixture, where the electrolyte is injected through the top cover, and oxygen is introduced through internal channels in the top cover, dissolving in the electrolyte. The focal point of this study is that stacked dual-layer CNT electrodes serve as sites for electrochemical reactions. The discharge curves corresponding to the experiments conducted with DMSO and TEGDME solvents are depicted in Fig. 1b. The discharge plateau of the DMSO solvent is observed at 2.8 V, surpassing that of the TEGDME solvent. Furthermore, the initial discharge capacity of the DMSO solvent is noteworthy at 6.7 mAh/cm, whereas the TEGDME solvent has an initial discharge capacity of 5.9 mAh/cm. The experimental results indicate a more pronounced advantage in battery discharge performance exhibited by the DMSO solvent, which is characterized by a higher discharge plateau and a greater initial discharge capacity.

The linear sweep voltammetry (LSV) curves of the electrodes in an O_2 atmosphere are displayed in Fig. 1d. The voltage interval tested was 2–3.2 V with a sweep rate of 0.5 mV/s. The DMSO solvent demonstrated a higher onset potential for the oxygen reduction reaction (ORR), approximately 2.8 V, surpassing that of the TEGDME solvent (2.7 V). The reduction peak for the TEGDME solvent occurs at 2.5 V, whereas the reduction peak for the DMSO solvent appears at 2.75 V, exceeding that of the TEGDME solvent. Furthermore, the DMSO solvent demonstrated a greater polarization current potential than did the TEGDME solvent, indicating that the reaction rate was significantly greater in the TEGDME solvent battery than in the DMSO battery.

Electrochemical impedance spectroscopy (EIS) spectra of different solvents are shown in Fig. 2a and b. The impedance data are fitted as shown in Table 1. On the basis of the EIS spectra and fitted data, the LOB obtained using DMSO as the solvent exhibited a smaller intermediate frequency semicircle before discharge, indicating a lower charge transfer impedance and a faster electron transfer rate conducive to the progress of the reaction. Although the charge transfer impedance of the DMSO solvent increases after discharge, it remains lower than that of the TEGDME solvent. The charge transfer impedance for the TEGDME solvent shows minimal variation throughout the discharge process, and there is no significant increase in the diffusion impedance.

XRD was used to analyze the discharge products on the CNT cathodes on both the inlet and the separator sides for the

CSTR: 32290.14.JUSTC-2024-0035
DOI: 10.52396/JUSTC-2024-0035
JUSTC, **2025**, 55(2): 0204

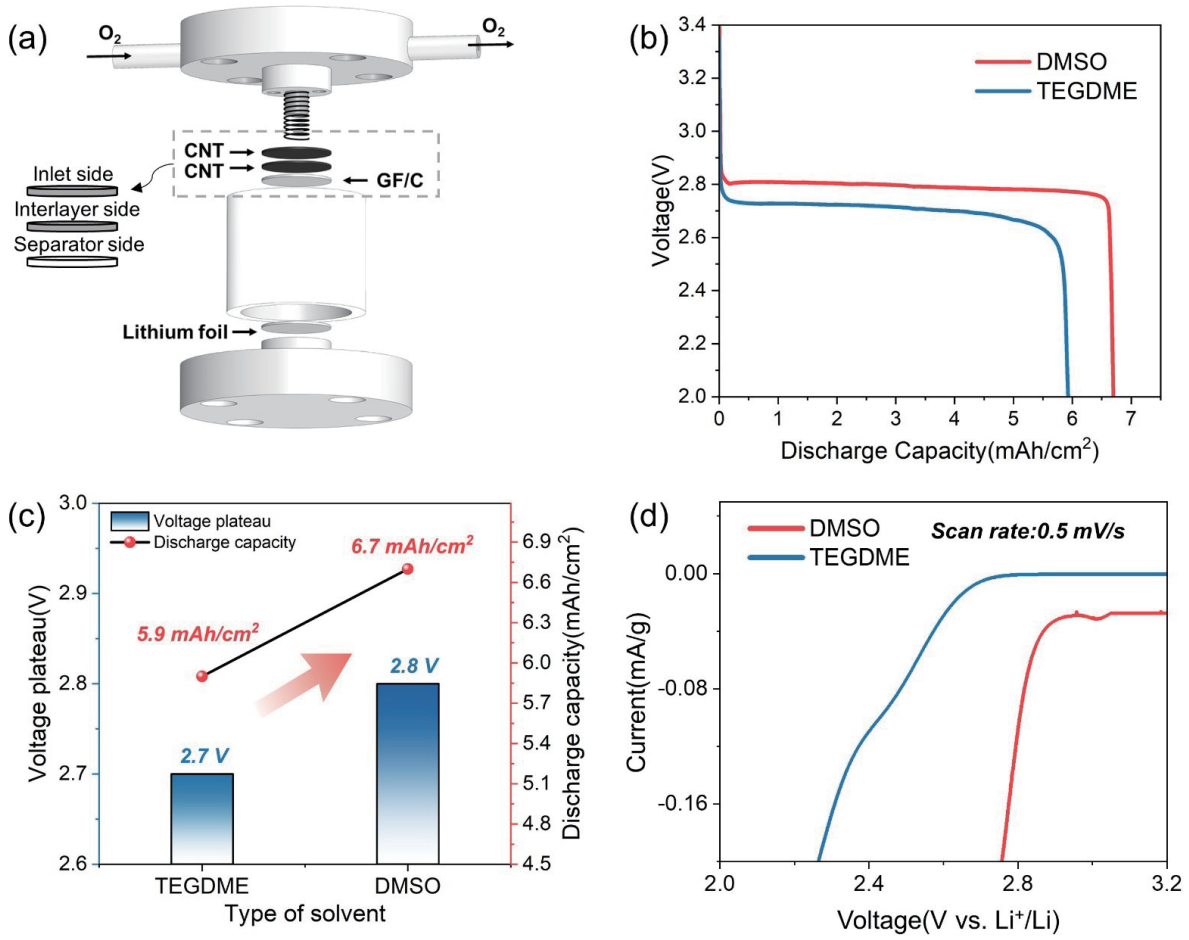

Fig. 1. (a) Diagram of the LOB with a Swagelok-type test device. (b) Capacity–voltage curves at 0.05 mA·cm^{-2} in different electrolyte solvents. (c) Comparison of the voltage plateau and discharge capacity in different electrolyte solvents. (d) LSV curves.

DMSO and TEGDME solvents. According to the XRD results, the predominant discharge product obtained using the DMSO solvent is Li_2O_2, with a small amount of LiOH byproduct. As previously proposed[37,38], the formation of LiOH can be attributed to a chemical reaction between water in the electrolyte and the discharged product Li_2O_2, which lacks evidence because the Karl Fischer titration of the $LiClO_4$/DMSO electrolyte revealed a shallow water content (<2E–5). Younesi et al.[39] reported the decomposition of DMSO by Li_2O_2, resulting in the generation of LiOH. Kwabi et al.[40] reported that the chemical reactivity of DMSO with Li_2O_2 and superoxide-like species leads to the generation of LiOH and $DMSO_2$, which can explain the XRD results when the $LiClO_4$/DMSO electrolyte is used. Furthermore, the XRD signals of the CNT electrode on the inlet side are more pronounced than those on the other sides are, indicating that the crystallinity of Li_2O_2 is greater than that of the other sides[41]. As illustrated in Fig. 3a, Li_2O_2 on the inlet side manifests as large layered structures, whereas on the separator side, it presents an amorphous film-like structure with lower crystallinity. The SEM results corroborate well with the XRD findings. In contrast to DMSO, as depicted in Fig. 2d, the discharge product in LOB using the TEGDME solvent is Li_2O_2 without significant LiOH byproducts. Both DMSO and TEGDME interfere with the carbon peaks in the XRD curves, which is attributed to the presence of CNTs. The cathodic XRD curve of the TEGDME solvent mirrors that of DMSO, with the signal peak on the inlet side being more intense, indicative of greater product crystallinity.

As shown in Fig. 3, the SEM images of each layer of the CNT cathodes in the LOB using DMSO exhibit distinct morphologies of the discharge products. On the inlet side of the CNT cathode, the predominant morphology of the discharge products (Li_2O_2) consists of spherical clusters formed by the accumulation of layered structures, as depicted in Fig. 3a, which is determined by the solution mechanism. Fig. 3b, c displays the morphologies of the discharge products on the interlayer sides of the dual-layer CNT cathode. In contrast to the clustered morphology observed on the inlet side, these discharge products are loosely stacked in a layered fashion, almost covering the electrode surface. The interlayers between the upper and lower electrode layers exhibit similar morphologies, as both layers are densely compressed during discharge, maintaining a uniform oxygen concentration. Fig. 3d shows the discharge products on the separator side of the CNT electrode, where significant differences appear due to the low oxygen concentration caused by excessive mass transfer resistance. Li_2O_2 does not form crystalline layered structures; instead, it manifests as amorphous, film-like products covering the electrode surface, induced by a surface

CSTR: 32290.14.JUSTC-2024-0035
DOI: 10.52396/JUSTC-2024-0035
JUSTC, **2025**, 55(2): 0204

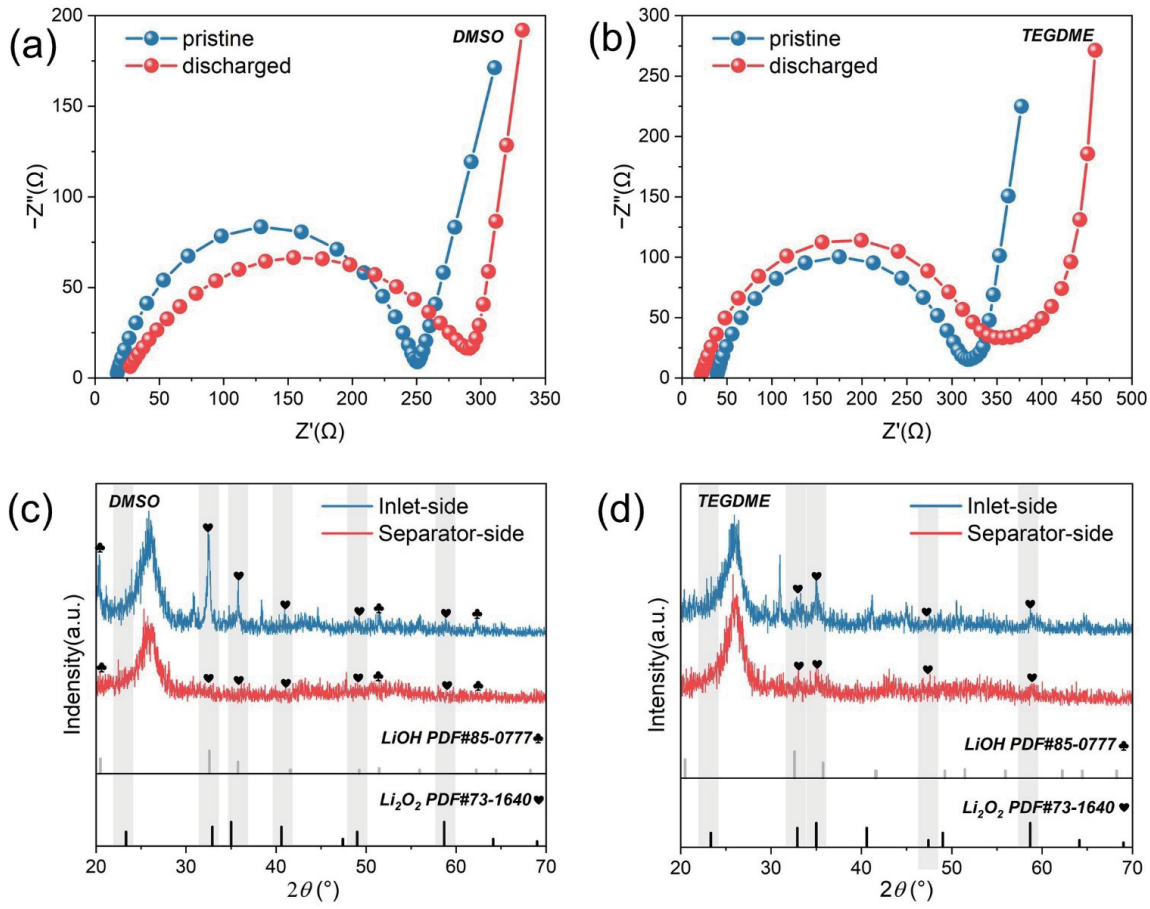

Fig. 2. (a) EIS spectra in different states with the DMSO solvent. (b) EIS spectra in different states with the TEGDME solvent. (c) XRD patterns of the different sides of the CNT electrode in DMSO. (d) XRD patterns of the CNT electrode on different sides with the TEGDME solvent.

Table 1. Impedance values before (R_Ω, R_{ct}) and after discharge (R_Ω', R_{ct}'); all units are in Ω·m.

Solvent types	R_Ω	R_{ct}	R_Ω'	R_{ct}'
DMSO	17.3	232.2	27.3	264.0
TEGDME	39.2	281	22.0	333.2

mechanism. Zhang et al.[42] utilized an ordered porous anodic aluminum oxide (AAO) electrode to investigate the distribution of discharge products within the cathode. The results indicate that with sufficiently large pore sizes, the size of the products on the oxygen side exceeds that on the separator side, which is consistent with our experimental results.

Most studies posit that the solution and surface mechanisms in LOB can be regulated through an electrolyte system[32,43] where solvents with high DN values, such as DMSO, induce the solution mechanism, whereas solvents with low DN values, such as TEGDME, induce the surface mechanism. However, our experimental results reveal a novel pathway for reaction mechanism induction in which the mechanism varies with the spatial position of the electrode. In DMSO, a layered appearance of solution mechanism products, transition state products, and surface mechanism products emerges as the spatial distribution of the electrode progresses. This phenomenon is attributed to the significant increase in the mass transfer resistance as the spatial position of the electrode changes. Dutta et al.[36] investigated the rate performance and primary limiting factors of LOB through a dual-layer electrode structure and reported that the limitation of oxygen diffusion was the cause of battery capacity decay. Owing to the sluggish kinetics of the cathodic reaction in LOB[44], the primary limiting factor during discharge is the transfer rate of active species, namely, the oxygen concentration distribution. A higher oxygen concentration on the inlet side corresponds to the solution mechanism, wherein products grow in the solution via LiO_2 disproportionation to form Li_2O_2, followed by a chemical reaction with DMSO and superoxide-like species to transform into LiOH. With a diluted oxygen concentration, a surface mechanism is induced on the separator side, resulting in amorphous film-like products that cover and block the electrode surface.

Fig. 4 shows SEM images of the CNT cathode in LOBs obtained using TEGDME, revealing significant differences from those obtained with DMSO. According to the XRD results, the discharge product of LOBs with TEGDME is Li_2O_2. On the inlet side, the discharge product forms a toroidal structure covering the entire electrode surface, representing a typical morphology characteristic of the solution mechanism, as depicted in Fig. 4a. Notably, large sheet-like products appear in the interlayers of the dual-layer CNTs. Unlike DMSO, these sheet-like Li_2O_2 structures are not stacked but rather scattered across the electrode surface. Owing to the increase in mass

CSTR: 32290.14.JUSTC-2024-0035
DOI: 10.52396/JUSTC-2024-0035
JUSTC, **2025**, 55(2): 0204

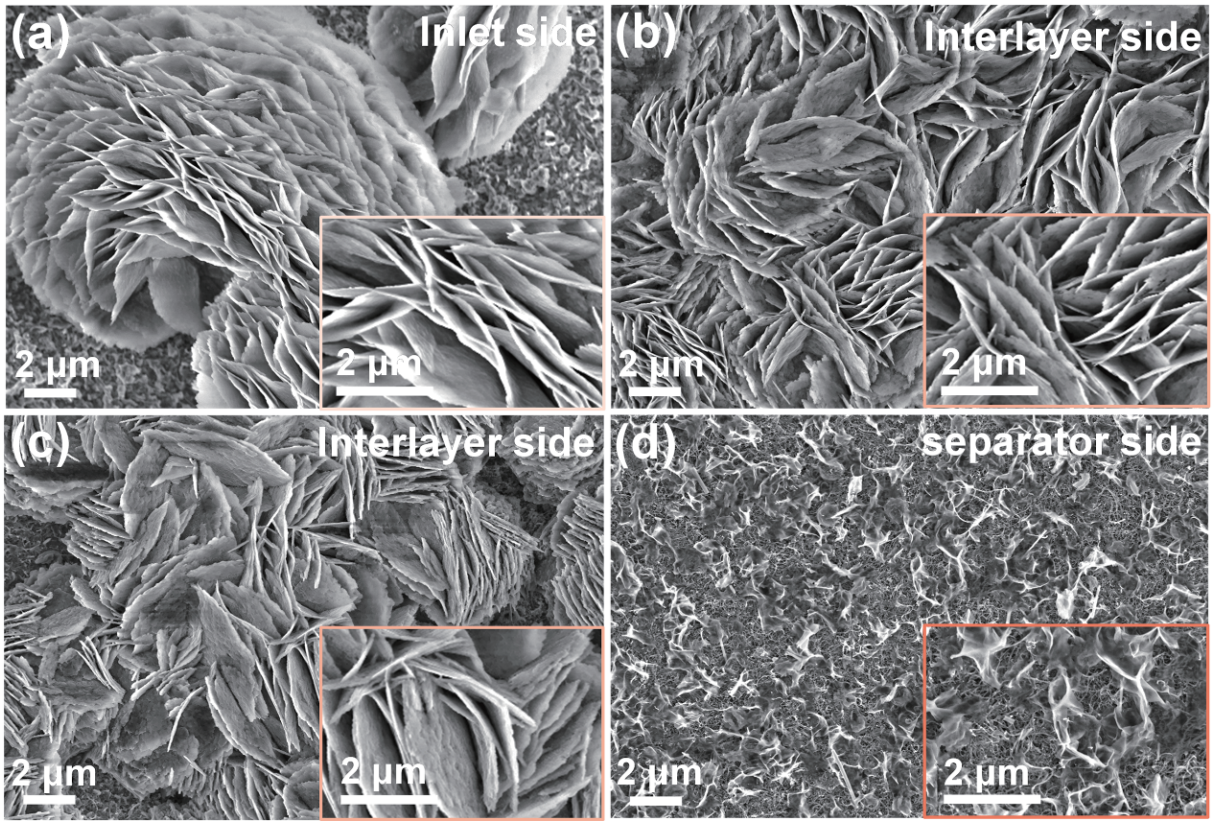

Fig. 3. SEM images of the dual-layer CNT cathode with DMSO: (a) inlet side, (b, c) interlayer side, and (d) separator side.

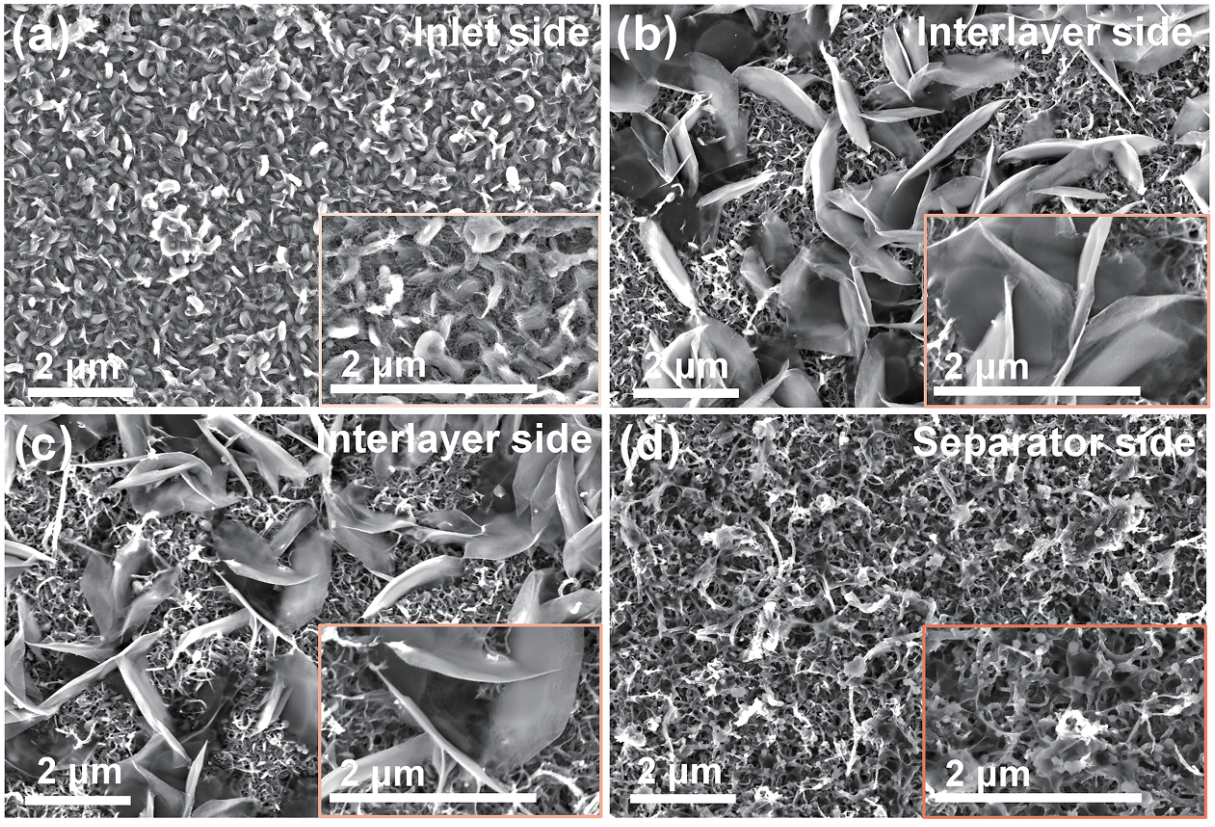

Fig. 4. SEM images of the dual-layer CNT cathode with TEGDME solvent: (a) inlet side, (b, c) interlayer side, and (d) separator side.

CSTR: 32290.14.JUSTC-2024-0035
DOI: 10.52396/JUSTC-2024-0035
JUSTC, **2025**, 55(2): 0204

transport resistance, the O_2 concentration on the interlayer side is lower than that on the inlet side. Therefore, the discharge products sharply decrease in quantity and cannot fully cover the electrode surface, in which these reduced scattered toroidal products stack and aggregate to form large-sized sheet-like Li_2O_2, as depicted in Fig. 4b, c. Fig. 4d shows film-like products on the CNT electrode closer to the separator side, following a surface mechanism growth path. This result aligns closely with the conclusion drawn from the use of DMSO as a solvent, indicating that the product morphology significantly varies with the oxygen concentration on the different surfaces of the CNT layers. Disproportionation reactions are induced by high oxygen concentrations, leading to the formation of large crystalline products. Conversely, a low oxygen concentration induces a surface mechanism, resulting in the formation of noncrystalline film-like products. However, the notable difference lies in the transition-state products, which assume a sheet-like morphology and exhibit substantial differences in shape and size compared with the crystalline toroidal products on the inlet side.

On the basis of the experimental results mentioned above, a schematic diagram illustrating the reaction pathways of LOB influenced by different solvents is provided in Fig. 5. The dual-layer CNT electrode resists material transport, leading to a significant concentration gradient of the active species. As evident from the morphologies of the discharge products, distinctive discharge reaction pathways are induced by different reaction interfaces. The slow diffusion of active species in the electrolyte, such as oxygen, results in the highest oxygen concentration gradient on the inlet side. The distribution of oxygen concentration gradients dominates the reaction pathways. The discharge products on the inlet side, when TEGDME is used, exhibit the characteristics of a solution mechanism, with LiO_2 forming toroidal Li_2O_2 in the electrolyte through a disproportionation reaction.

In contrast, when DMSO is used as the solvent, Li_2O_2 generated through a solution mechanism forms large spherical clusters composed of stacked layers. For the interlayers of the dual-layer CNT electrode, the discharge product morphology consisted of layers growing vertically on the electrode surface, exhibiting the same pattern in both the DMSO and TEGDME solvents. On the separator side, where the oxygen concentration is shallow, the discharge product is amorphous, displaying characteristics of a surface mechanism; this product grows on the electrode surface and covers the active sites with a film-like morphology. Our experimental findings reveal a significant deviation from the prevailing viewpoint, where under identical reaction conditions, the reaction mechanism undergoes noticeable variations corresponding to the spatial distribution of the electrode.

Furthermore, the physical properties of TEGDME and DMSO, which are electrolyte solvents with significant differences, exhibit substantial variations in discharge products and morphologies. Notably, when TEGDME is used as the solvent in LOB, the discharge product is Li_2O_2, whereas when DMSO is used, the discharge product is Li_2O_2, and a small amount of LiOH is present, which is the byproduct of the chemical reactivity of DMSO with Li_2O_2 and superoxide-like species[40]. Parameters such as the DN, oxygen diffusion rate, and oxygen solubility, provided in Fig. 5, highlight the considerable differences between the two solvents. A model built by Rauter et al.[35] revealed that the initial oxygen concentration of LOB obtained using TEGDME as the solvent was greater than that obtained using DMSO. Moreover, the attenuation rate was greater when TEGDME was used as the solvent inside the electrode. In addition, the volume fraction of the product obtained using DMSO was much greater than that obtained using TEGDME, which is consistent with our experimental results. The higher oxygen diffusion rate in DMSO indicates superior transport characteristics compared with those of TEGDME. Compared with their discharge products, the size of the discharge products in DMSO is significantly greater because the high oxygen concentration induces a solution mechanism. Therefore, comparing TEGDME and DMSO as typical solvents for LOB electrolytes emphasizes the regulatory role of solvent mass transport properties in dictating reaction pathways.

4 Conclusions

In this work, we investigated the impact of two electrolyte solvents in LOBs on the discharge capacity, product

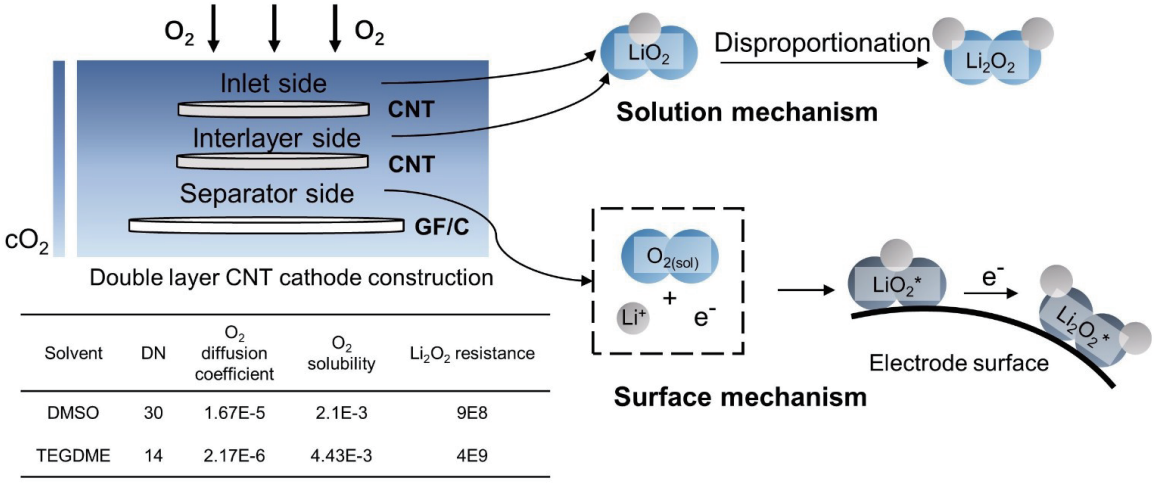

Solvent	DN	O_2 diffusion coefficient	O_2 solubility	Li_2O_2 resistance
DMSO	30	1.67E-5	2.1E-3	9E8
TEGDME	14	2.17E-6	4.43E-3	4E9

Fig. 5. Schematic diagram of the mechanism of the reaction pathways in LOBs.

CSTR: 32290.14.JUSTC-2024-0035
DOI: 10.52396/JUSTC-2024-0035
JUSTC, **2025**, 55(2): 0204

morphology, and reaction pathways. DMSO, a high-DN-value electrolyte solvent, is believed to induce solution pathways, whereas TEGDME induces surface pathways. In contrast, our experimental results indicate that both solution and surface pathways coexist under the influence of DMSO. Moreover, the reaction pathways are influenced by the internal spatial position of the electrode, and similar conclusions are drawn with respect to the TEGDME solvent. The dual-electrode structure involves the utilization of two identical CNT electrodes, which are stacked and employed as a single electrode that participates in electrochemical reactions, thereby allowing for an increase in mass transfer resistance. On the basis of the discharge product morphology on each layer of the CNT electrode, the discharge products near the inlet exhibit characteristics indicative of a solution mechanism, whereas the discharge products near the separator present features associated with a surface mechanism. The morphology of the discharge products between the layers of CNTs remains consistent. The transfer of active species within the battery is notably sluggish, resulting in a significantly higher oxygen concentration on the air inlet side than on the separator side. A greater oxygen concentration induces a solution mechanism.

Furthermore, a comparative analysis of the discharge products between DMSO and TEGDME revealed that, owing to its superior mass transport characteristics, DMSO results in larger discharge product sizes and higher discharge capacity than TEGDME. We assert that the impact of solvents on the reaction pathways during the discharge process, in addition to DN values, should not disregard the influence of mass transport properties. This work presents a distinct perspective on how solvents influence discharge products and reaction pathways, contributes to the understanding of mass transfer mechanisms, and offers a new approach for regulating reaction pathways.

Acknowledgements

This work was supported by the National Natural Science Foundation of China (52376080 and 52306122), the Anhui Provincial Natural Science Foundation (2308085QE174), the China Postdoctoral Science Foundation (2023TQ0346), the Postdoctoral Fellowship Program of CPSF (GZC20232522), the Fundamental Research Funds for the Central Universities (WK2090000057), and the Students' Innovation and Entrepreneurship Foundation of USTC (CY2023C008).

Conflict of interest

The authors declare that they have no conflict of interest.

Biographies

Aijing Yan is pursuing a master's degree at the University of Science and Technology of China. She graduated from Nanjing Normal University with a bachelor's degree. Her research mainly focuses on multi-component assisted mass transfer in lithium-gas batteries.

Xu Xiao is currently a Postdoctoral Researcher in the Department of Thermal Science and Energy Engineering at the University of Science and Technology of China (USTC). She received her Ph.D. degree from USTC in 2022. Her research mainly focuses on the material transport characteristics and energy-quality conversion processes in lithium-gas batteries.

Peng Tan is currently the Executive Director and Doctoral Supervisor of the Department of Thermal Science and Energy Engineering, the University of Science and Technology of China. He received his Ph.D. degree from the Hong Kong Polytechnic University in 2016. His research mainly focuses on the common multi-field coupling energy transmission and transformation problems in electrochemical energy storage systems, including the exploration of multi-field coupling transmission mechanism, theoretical model construction and regulatory mechanism research.

References

[1] Wen J, Zhao D, Zhang C. An overview of electricity powered vehicles: Lithium-ion battery energy storage density and energy conversion efficiency. *Renewable Energy*, **2018**, *162*: 1629–1648.
[2] Xu J, Cai X, Cai S, et al. High-energy lithium-ion batteries: Recent progress and a promising future in applications. *Energy & Environmental Materials*, **2023**, *6*: e12450.
[3] Shi M, Ren Y, Cao J, et al. Current situation and development prospects of discharge pretreatment during recycling of lithium-ion batteries: A review. *Batteries & Supercaps*, **2024**, *7*: e202300477.
[4] He W, Guo W, Wu H, et al. Challenges and recent advances in high capacity Li-rich cathode materials for high energy density lithium-ion batteries. *Advanced Materials*, **2021**, *33*: e2005937.
[5] Cao D, Bai Y, Zhang J, et al. Irreplaceable carbon boosts Li-O_2 batteries: From mechanism research to practical application. *Nano Energy*, **2021**, *89*: 106464.
[6] Farooqui U R, Ahmad A L, Hamid N A. Challenges and potential advantages of membranes in lithium air batteries: A review. *Renewable and Sustainable Energy Reviews*, **2017**, *77*: 1114–1129.
[7] Zhou Y, Guo S. Recent advances in cathode catalyst architecture for lithium–oxygen batteries. *eScience*, **2023**, *3*: 100123.
[8] Padbury R, Zhang X. Lithium–oxygen batteries: Limiting factors that affect performance. *Journal of Power Sources*, **2011**, *196*: 4436–4444.
[9] Jung K N, Kim J, Yamauchi Y, et al. Rechargeable lithium–air batteries: A perspective on the development of oxygen electrodes. *Journal of Materials Chemistry A*, **2016**, *4*: 14050–14068.
[10] Kwak W J, Rosy, Sharon D, et al. Lithium-oxygen batteries and related systems: Potential, status, and future. *Chemical Reviews*, **2020**, *120*: 6626–6683.
[11] Lu Y C, Gallant B M, Kwabi D G, et al. Lithium–oxygen batteries: Bridging mechanistic understanding and battery performance. *Energy & Environmental Science*, **2013**, *6*: 750–768.
[12] Chen Y, Gao X, Johnson L R, et al. Kinetics of lithium peroxide oxidation by redox mediators and consequences for the lithium-oxygen cell. *Nature Communications*, **2018**, *9*: 767.
[13] Wu X, Niu B, Zhang H, et al. Enhancing the reaction kinetics and reversibility of Li–O_2 batteries by multifunctional polymer additive. *Advanced Energy Materials*, **2023**, *13*: 2203089.
[14] Kundu D, Black R, Adams B, et al. A highly active low voltage redox mediator for enhanced rechargeability of lithium-oxygen batteries. *ACS Central Science*, **2015**, *1*: 510–515.
[15] Wan H, Sun Y, Cai W, et al. A friendly soluble protic additive enabling high discharge capability and stabilizing Li metal anodes in Li–O_2 batteries. *Advanced Functional Materials*, **2022**, *32*: 2106984.
[16] Xia C, Kwok C Y, Nazar L F. A high-energy-density lithium-oxygen battery based on a reversible four-electron conversion to lithium oxide. *Science*, **2018**, *361*: 777–781.
[17] Shui J L, Okasinski J S, Kenesei P, et al. Reversibility of anodic lithium in rechargeable lithium-oxygen batteries. *Nature Communications*, **2013**, *4*: 2255.

CSTR: 32290.14.JUSTC-2024-0035
DOI: 10.52396/JUSTC-2024-0035
JUSTC, **2025**, 55(2): 0204

[18] Lin X, Sun Z, Tang C, et al. Highly reversible O_2 conversions by coupling LiO_2 intermediate through a dual-site catalyst in Li-O_2 batteries. *Advanced Energy Materials*, **2020**, *10*: 2001592.
[19] Li F, Chen J. Mechanistic evolution of aprotic lithium-oxygen batteries. *Advanced Energy Materials*, **2017**, *7*: 1602934.
[20] Xiong Q, Huang G, Zhang X B. High-capacity and stable Li-O_2 batteries enabled by a trifunctional soluble redox mediator. *Angewandte Chemie International Edition*, **2020**, *59*: 19311–19319.
[21] Shen Z Z, Zhou C, Wen R, et al. Surface mechanism of catalytic electrodes in lithium-oxygen batteries: How nanostructures mediate the interfacial reactions. *Journal of the American Chemical Society*, **2020**, *142*: 16007–16015.
[22] Li R, Hu A, Zhao C, et al. Tailoring mixed geometrical configurations in amorphous catalysts to activate oxygen electrode reactions of lithium-oxygen batteries. *Chemical Engineering Journal*, **2023**, *452*: 139162.
[23] Huang Q, Dang F, Zhu H, et al. A hierarchical porous carbon supported Pd@Pd4S heterostructure as an efficient catalytic material positive electrode for Li–O_2 batteries. *Journal of Power Sources*, **2020**, *451*: 227738.
[24] Ko Y, Park H, Lee K, et al. Anchored mediator enabling shuttle-free redox mediation in lithium-oxygen batteries. *Angewandte Chemie (International Ed)*, **2020**, *59*: 5376–5380.
[25] Zhao H, Chi Z, Kong D, et al. Constructing *in situ* $SOCl_2$-induced protective layer on Li anode for high-performance Li–O_2 batteries containing LiI redox mediator. *Chemical Engineering Journal*, **2023**, *469*: 143962.
[26] Lin X D, Gu Y, Shen X R, et al. An oxygen-blocking oriented multifunctional solid–electrolyte interphase as a protective layer for a lithium metal anode in lithium–oxygen batteries. *Energy & Environmental Science*, **2021**, *14*: 1439–1448.
[27] Li R, Fan Y, Zhao C, et al. Air-stable protective layers for lithium anode achieving safe lithium metal batteries. *Small Methods*, **2023**, *7*: e2201177.
[28] Xu W, Viswanathan V V, Wang D, et al. Investigation on the charging process of Li_2O_2-based air electrodes in Li–O_2 batteries with organic carbonate electrolytes. *Journal of Power Sources*, **2011**, *196*: 3894–3899.
[29] Jethwa R B, Mondal S, Pant B, et al. To DISP or not? The far-reaching reaction mechanisms underpinning lithium-air batteries. *Angewandte Chemie International Edition*, **2024**, *63*: e202316476.
[30] Freunberger S A, Chen Y, Peng Z, et al. Reactions in the rechargeable lithium-O_2 battery with alkyl carbonate electrolytes. *Journal of the American Chemical Society*, **2011**, *133*: 8040–8047.
[31] Wu Z, Tian Y, Chen H, et al. Evolving aprotic Li-air batteries. *Chemical Society Reviews*, **2022**, *51*: 8045–8101.
[32] Johnson L, Li C, Liu Z, et al. The role of LiO_2 solubility in O_2 reduction in aprotic solvents and its consequences for Li-O_2 batteries. *Nature Chemistry*, **2014**, *6*: 1091–1099.
[33] Liu Y, Pérez-Luna V H, Prakash J. Quantitative elucidation of cathode reaction mechanisms in Li-O_2 batteries within high donor number solvents. *Electrochimica Acta*, **2024**, *475*: 143669.
[34] Christy M, Arul A, Zahoor A, et al. Role of solvents on the oxygen reduction and evolution of rechargeable Li-O_2 battery. *Journal of Power Sources*, **2017**, *342*: 825–835.
[35] Rauter M T, Augustin M, Spitthoff L, et al. Product formation during discharge: A combined modelling and experimental study for Li–O_2 cathodes in LiTFSI/DMSO and LiTFSI/TEGDME electrolytes. *Journal of Applied Electrochemistry*, **2021**, *51*: 1437–1447.
[36] Dutta A, Ito K, Kubo Y. Establishing the criteria and strategies to achieve high power during discharge of a Li–air battery. *Journal of Materials Chemistry A*, **2019**, *7*: 23199–23207.
[37] Geaney H, O'Dwyer C. Electrochemical investigation of the role of MnO_2 nanorod catalysts in water containing and anhydrous electrolytes for Li-O_2 battery applications. *Physical Chemistry Chemical Physics*, **2015**, *17*: 6748–6759.
[38] Meini S, Piana M, Tsiouvaras N, et al. The effect of water on the discharge capacity of a non-catalyzed carbon cathode for Li-O_2 batteries. *Electrochemical and Solid-State Letters*, **2012**, *15*: A45.
[39] Younesi R, Norby P, Vegge T. A new look at the stability of dimethyl sulfoxide and acetonitrile in Li-O_2 batteries. *ECS Electrochemistry Letters*, **2014**, *3*: A15–A18.
[40] Kwabi D G, Batcho T P, Amanchukwu C V, et al. Chemical instability of dimethyl sulfoxide in lithium-air batteries. *The Journal of Physical Chemistry Letters*, **2014**, *5*: 2850–2856.
[41] Liang H, Jia L, Chen F. Three-dimensional self-standing Co@NC octahedron/biochar cathode for non-aqueous Li-O_2 batteries: Efficient catalysis for reversible formation and decomposition of LiOH. *Journal of Materials Science*, **2020**, *55*: 7792–7804.
[42] Zhang Z, Xiao X, Yu W, et al. Reacquainting the sudden-death and reaction routes of Li–O_2 batteries by *ex situ* observation of Li_2O_2 distribution inside a highly ordered air electrode. *Nano Letters*, **2022**, *22*: 7527–7534.
[43] Zhu M, Li M, Lian Y, et al. Direct observation of solvent donor number effect on lithium–oxygen battery capacity via a nanoarray cathode model. *The Journal of Physical Chemistry C*, **2022**, *126*: 10248–10257.
[44] Zhang S, Qiu J, Zhang Y, et al. Crystal phase conversion on cobalt oxide: Stable adsorption toward LiO_2 for film-like discharge products generation in Li-O_2 battery. *Small*, **2022**, *18*: e2201150.

CSTR: 32290.14.JUSTC-2024-0035
DOI: 10.52396/JUSTC-2024-0035
JUSTC, **2025**, 55(2): 0204